



## Novel technique to study the wet chemical etching response of multi-crystalline silicon wafers

Vladyslav Matkivskiy<sup>a,\*</sup>, Arne Karstein Røyset<sup>c</sup>, Gaute Stokkan<sup>b</sup>, Pål Tetlie<sup>b</sup>,  
Marisa Di Sabatino<sup>a</sup>, Gabriella Tranell<sup>a,\*</sup>

<sup>a</sup> NTNU, Alfred Getz' vei 2B, Trondheim 7034, Norway

<sup>b</sup> SINTEF, Alfred Getz' vei 2B, Trondheim 7034, Norway

<sup>c</sup> SINTEF, Høgskoleringen 5, Trondheim 7034, Norway

### ABSTRACT

The current work aimed to demonstrate the application of a technique where white light interferometry (WLI) and Laue X-ray crystallography scanner characterisation were combined to study the chemical etching response of diamond cut multi-crystalline Si (mc-Si) wafers. Using this technique, the effect of different texturing additives (isopropyl alcohol, sodium hypochlorite) was evaluated by examining the topography of the mc-Si surfaces before and after etching. The etching responses of monocrystalline Si wafers of (100), (110) and (111) orientations were used as reference for comparison with the multi-crystalline wafers investigated. The texturing results illustrated the influence of different crystal-orientations on the etching rate. It was revealed that for the mc-Si wafers, the etching speed of the different crystal grain-planes is increasing with their crystallographic similarity with the main (*hkl*) planes (100, 110, 111). The comparison of isopropyl alcohol (IPA) and sodium hypochlorite (NaOCl) additives to KOH solutions showed that NaOCl additive is favourable for the polishing of mc-Si wafers, while IPA can be used as polishing only for crystal grains close to the (111) orientation.

### 1. Introduction

Crystalline Si wafer-based photovoltaics (PV) dominate the global solar cell (SC) market with 89.3 % of the installed capacity in 2021 [1]. All published record research-cell efficiencies belong to monocrystalline HIT cells (Kaneka – 26.7 %) [2], while multi-crystalline (mc-Si) record cells have achieved efficiencies of up to 23.3 % (JinkoSolar) [2]. Cell types such as passivated emitter and rear cell (PERC) [3], dopant free with asymmetric hetero-contacts (DASH) [4], or heterojunction interdigitated back contact (HJ-IBC) [5], entering the market create new opportunities for mc-Si photovoltaic modules as these new cell types simplify the fabrication process and hence provide the basis for gaining new market positions. Additionally, the standard fabrication process for mc-Si photovoltaics has potential for improvement in operations such as wafer polishing, texturing and passivation [6].

The standard mc-solar cell fabrication process is generally lower in cost in comparison to the monocrystalline cells. Thus, the combination of mc-Si multi-wire diamond sawing (MWSS) [7] and novel cell types has a large potential for achieving general cost and efficiency improvements for the PV industry. Despite wide MWSS application, the downside to this sawing method is the deeper saw mark damage inflicted on the Si wafer surface. This damage results in Si material losses

due to the need for subsequent wafer polishing to remove this damaged layer. Therefore, it is important to implement new cost-effective wafer surface processing for the diamond cut mc-Si.

As polishing of Si wafers following ingot slicing is a key step in the solar cell fabrication process, different polishing techniques have been introduced. Industrially, the well-established chemical-mechanical polishing (CMP) process [8] is efficient and widely implemented for both mono- and mc-Si wafers. This process has both cost- and environmental hazard drawbacks as it involves the usage of mechanically abrasive particles such as alumina (Al<sub>2</sub>O<sub>3</sub>), silica (SiO<sub>2</sub>) and ceria (CeO<sub>2</sub>) [9], which contribute to particulate waste in water reservoirs if not properly separated.

A possible alternative to CMP was discussed in a previous study by Zhang et al [9] on mc-Si wafer surface polishing and texturing. These authors established that a solution of mixed sodium hydroxide (NaOH) and sodium hypochlorite (NaOCl) has a polishing effect on mc-wafers. Following these results, it was illustrated that it is possible to obtain cost-effective polishing solutions for diamond cut mc-Si wafers. As for mono-crystalline-Si wafers, surface polishing or texturing is based mainly on the use of different alkaline (potassium hydroxide (KOH) [10] or NaOH [11]) solutions or the more expensive and hazardous tetramethyl ammonium hydroxide (TMAH) [12]. Subsequently, it appears

\* Corresponding authors.

E-mail addresses: [vladyslav.matkivskiy@ntnu.no](mailto:vladyslav.matkivskiy@ntnu.no) (V. Matkivskiy), [gabriella.tranell@ntnu.no](mailto:gabriella.tranell@ntnu.no) (G. Tranell).

<https://doi.org/10.1016/j.mseb.2023.116343>

Received 30 August 2022; Received in revised form 9 January 2023; Accepted 28 January 2023

Available online 6 February 2023

0921-5107/© 2023 The Author(s). Published by Elsevier B.V. This is an open access article under the CC BY license (<http://creativecommons.org/licenses/by/4.0/>).

**Table 1**  
Recipes for polishing, cleaning and texturing treatments.

Process	Recipe & name	Volume Concentration (ml)	Etching time	Process temperature (°C)
Damage removal	“HNA” - HF:	80:300:250	5 min	room temperature
	“KOHpol” - KOH solution: IPA:NaOCl solution	800:20:10	10 min	85 °C
Etching	“KOHIPA” - KOH solution: IPA	800:80	5 and 15 min	85 °C
Etching	“KOHNa” - KOH solution:NaOCl solution	800:40	5 and 15 min	85 °C
Etching	“KOHmix” - KOH solution: IPA:NaOCl solution	800:80:40	5 min	85 °C

that not only alkaline based solutions are effective for the polishing of c-Si wafers. As an alternative, the first industrially implemented method of a mixed acid Si polish etching solution, called “CP4” [13], consisting of hydrofluoric (HF), nitric (HNO<sub>3</sub>) and acetic acid (CH<sub>3</sub>COOH) was used at room temperature.

Chemical texturing of Si wafers is an essential step in crystalline solar cell fabrication, aimed at improving light absorption of the Si wafer surface. Industry has access to texturing techniques such as laser texturing [14], reactive ion etching (RIE) [15] and metal assisted chemical etching (MACE) [16], with wet chemical texturing [17] being the widest implemented process. This approach is mainly based on the use of NaOH, KOH and TMAH solutions. Despite the low cost of alkaline based texturing, high surface texture symmetry and coverage is still challenging. A solution for this issue is chemical texturing with additives. Additives are surfactant agents which improve chemical texturing processes such as polishing, texturing and damage removal [11,18] and are typically of commercial, proprietary nature. Researchers, due to a lack of available information, tend to use alternative surfactants such as isopropyl alcohol (IPA) [19], and ethylene glycol [17]. IPA is well

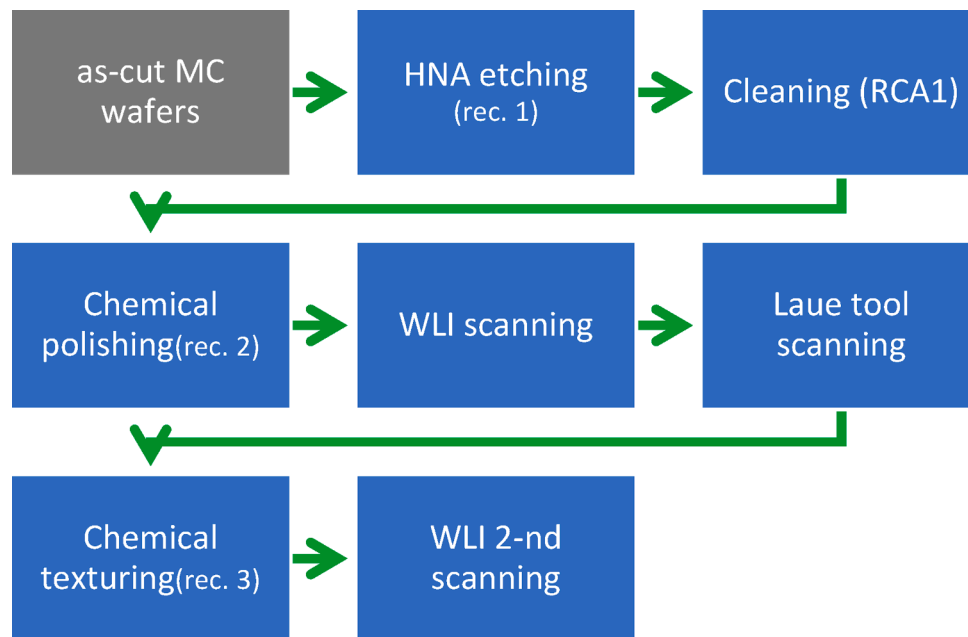


Fig. 1. Experimental flowchart.

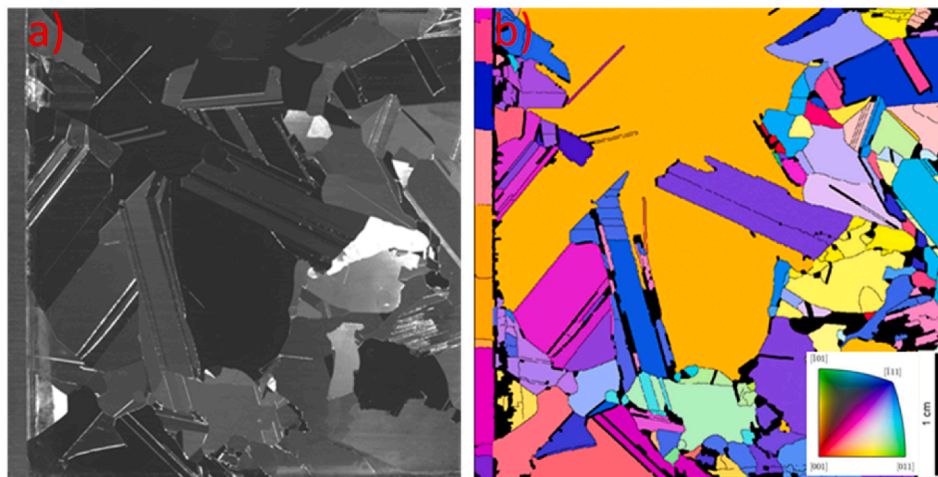


Fig. 2. A) optical scan of the sample a) b) laue tool created hkl map (colour represents hkl orientations) of the same sample.

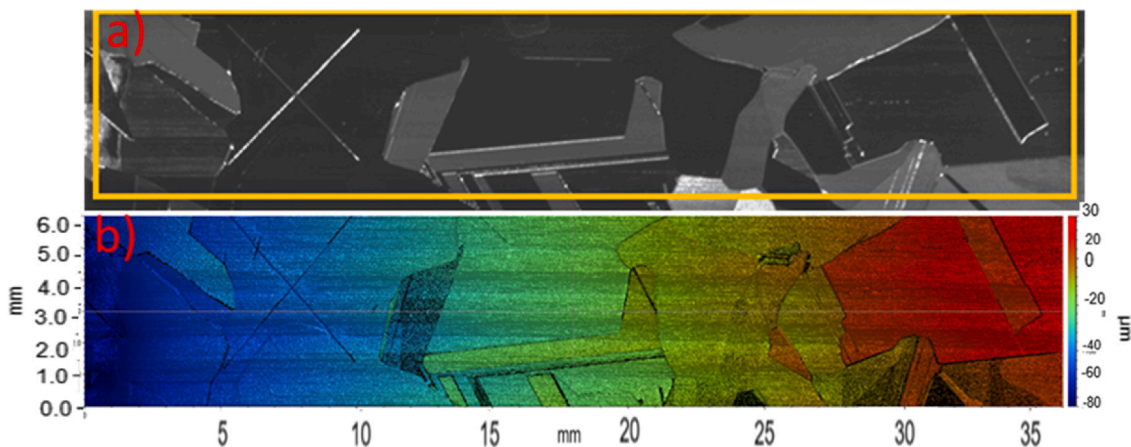


Fig. 3. A) optical scan of the sample a; b) wli scanned area (a) of the sample a (colour bar represents change in the topological height).

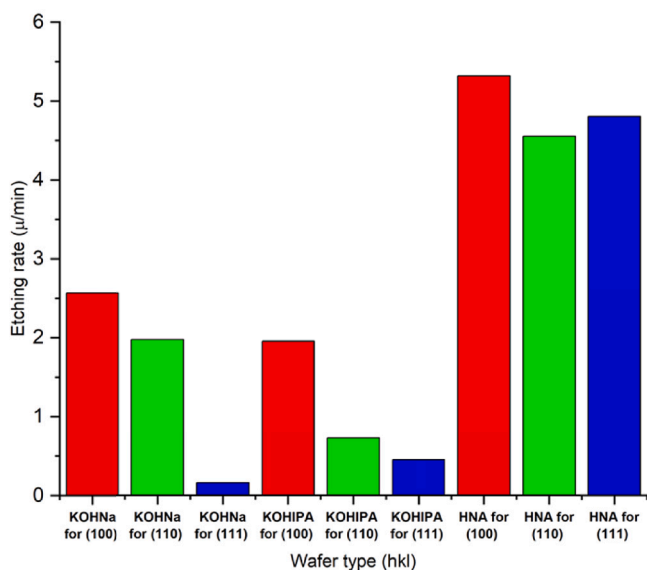


Fig. 4. Etching rates of different mono-crystal wafer orientations for different KOH-based solutions.

known as an additional surfactant in combination with TMAH or KOH chemical etchants. NaOCl is also reported as a surfactant for alkaline etching [19,20].

The aim of the current study is to demonstrate a new analysis approach, combining the Laue X-ray crystallography tool [21] and a white light interferometry (WLI) 3d-profilometer [22] to evaluate the chemical polishing and texturing responses of diamond-sawed mc-Si wafers. An important part of this work is the comparison of IPA and

NaOCl additives as supportive etching agents for KOH-based wet chemical etching in industrial applications [23].

## 2. Experimental

### 2.1. Materials

The current study was carried out on industrially diamond-cut p-type mc-Si wafers with a thickness of  $180 \pm 25 \mu\text{m}$ . Polished p-type SiMat mono-crystalline wafers of three main orientations, namely (111), (100), and (110), with a thickness of  $275 \pm 25 \mu\text{m}$ , were used as etching response references.

### 2.2. Experimental flowsheet

Si wafers were cut into  $4 \times 4 \text{ cm}$  pieces with a laser. As a first step, the wafers were cleaned in an RCA 1 solution with subsequent ethanol (99.8 %) immersion and drying. Further, the wafers were etched in the surface damage removal solution HNA (hydrofluoric, nitric, acetic acid according to recipe 1, Table 1). Following the HNA damage removal process, wafers were polished in a KOH based solution. After the damage removal process, the multi-crystalline wafers were scanned with the WLI and Laue tool, as described in section 2.3. Subsequently, wafers were chemically textured by one of three different KOH solutions with additives (Table 1). Lastly, the textured wafers were scanned again using WLI. A flowchart for the experiments is presented in Fig. 1 and further detailed in the sections below.

### 2.3. Chemical etching

The polishing treatment was based on a previous study [18] of MACE for HPMC (high-performance multicrystalline) wafers. A polishing effect

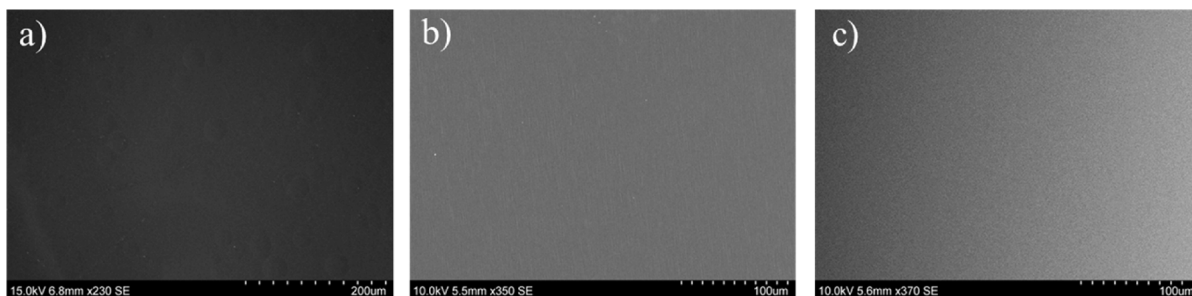


Fig. 5. SEM images of the mono-crystalline wafers etched in the solution with NaOCl additive (rec. "KOHNa"); a) (100) orientation, b) (110) orientation, c) (111) orientation.



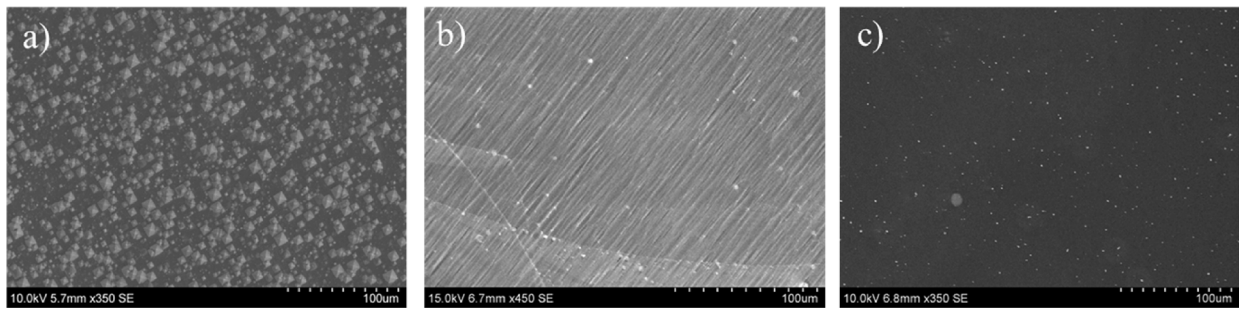


Fig. 6. SEM images of the mono-crystalline wafers etched in the solution with IPA additive (rec. "KOHIPA"); a) (100) orientation, b) (110) orientation, c) (111) orientation.

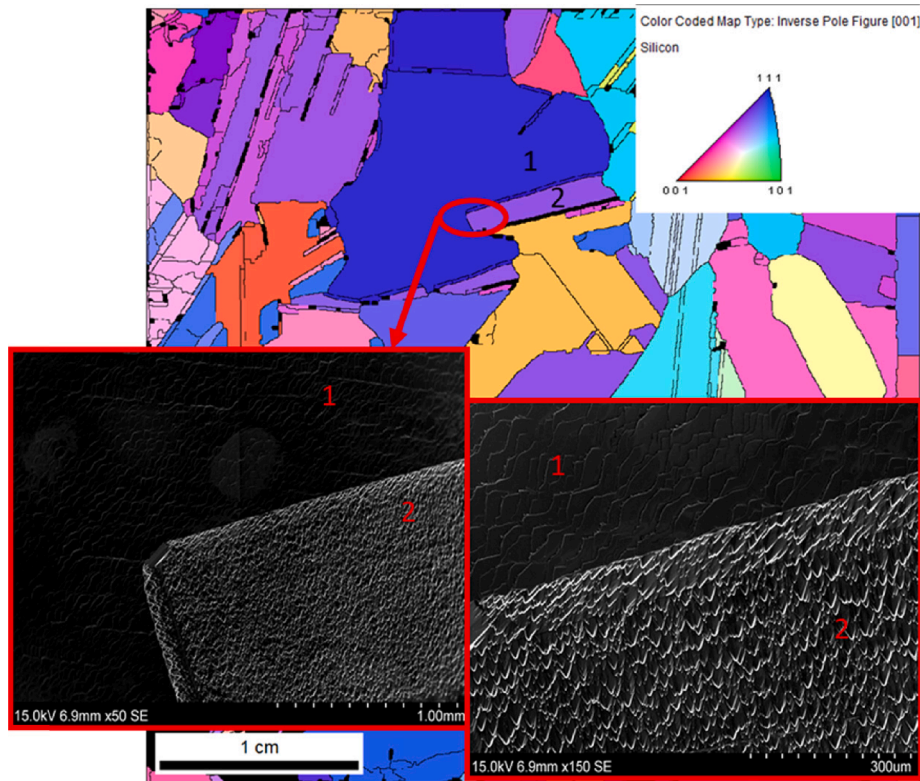


Fig. 7. SEM images combined with the LAUE mapping indicate a morphological effect of the NaOCl and IPA solution (rec. "KOHmix") for the multi-crystalline wafers.

was obtained by the application of NaOH/NaOCl solution prior to the MACE procedure. The first polishing procedure consisted of a treatment in HNA [24] solution (Table 1), which refers to the mixing of nitric ( $\text{HNO}_3$ ), acetic ( $\text{CH}_3\text{COOH}$ ) and hydrofluoric (HF) acids. The purpose of the HNA polishing is smoothness and removal of the waviness of the surface profile created by the wire movement. Next, a secondary polishing operation was carried out in a solution of low-concentration KOH mixed with NaOCl (concentrations are presented in the Table 1).

Following the chemical polishing (HNA polishing and KOH polishing), the mc-wafers were cleaned in the RCA 1 solution and characterized for individual crystal orientation by the Laue tool and for initial, relative crystal height difference by WLI (white light interferometry) as described in prior work [25]. Characterized wafers were subsequently chemically textured. Three parallel wafers for each experimental condition were treated and analysed.

KOHIPA solution was used to observe the IPA additive effect on the etching response of differently oriented grains on the multi-crystalline samples. Additionally, etching was conducted during 5 and 15 min for

"KOHIPA" and "KOHNa" recipes. Solution – "KOHmix", a mix of NaOCl and IPA additives was used in the etching experiments to investigate possible compensation or interaction between these additives.

The etching solution temperature was  $85^\circ\text{C}$ , in accordance with previous work of Zong et al [26], where NaOH/NaOCl solution polishing and alkaline texturing were applied for formation of nano-porous structures on the sample surface. In this work, a temperature drop (with a duration of 1–3 min) when samples were inserted into the solution was observed. Such temperature drop was noted for all etching solutions (KOHIPA, KOHNa, KOHmix, KOHpol) and can be explained as a result of short-term cooling of the solution by the immersion of the room temperature sample (holder).

#### 2.4. Measurements and analysis

The Laue X-ray crystallography scanner tool [21] is an alternative to the widely implemented electron backscatter diffraction (EBSD) technique. This technique is preferable in situations when large area samples



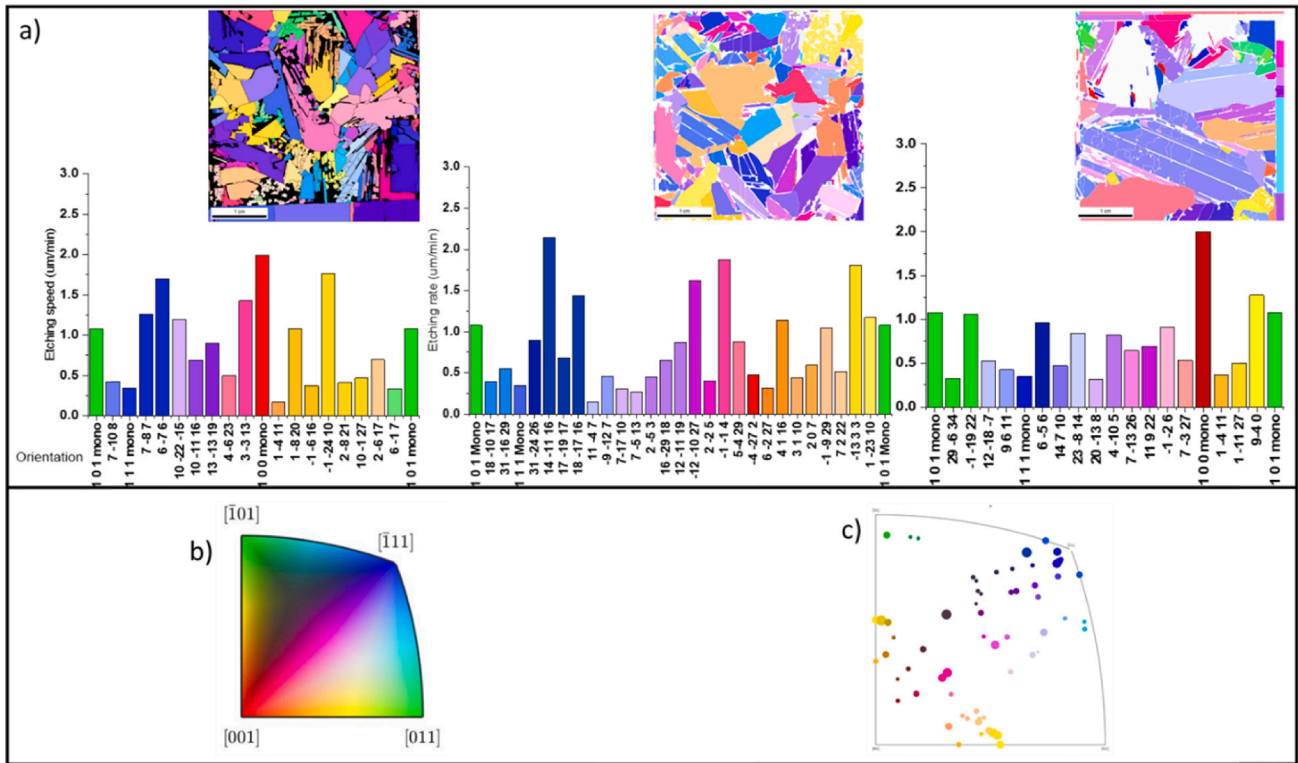


Fig. 8. a) Colour key; b) Etching rate (circle size) diagram per grain distribution for different orientations calculated from the samples; c) Etching rate per grain for each sample individually; for the recipe “KOHIPA” with 5 min etching time.

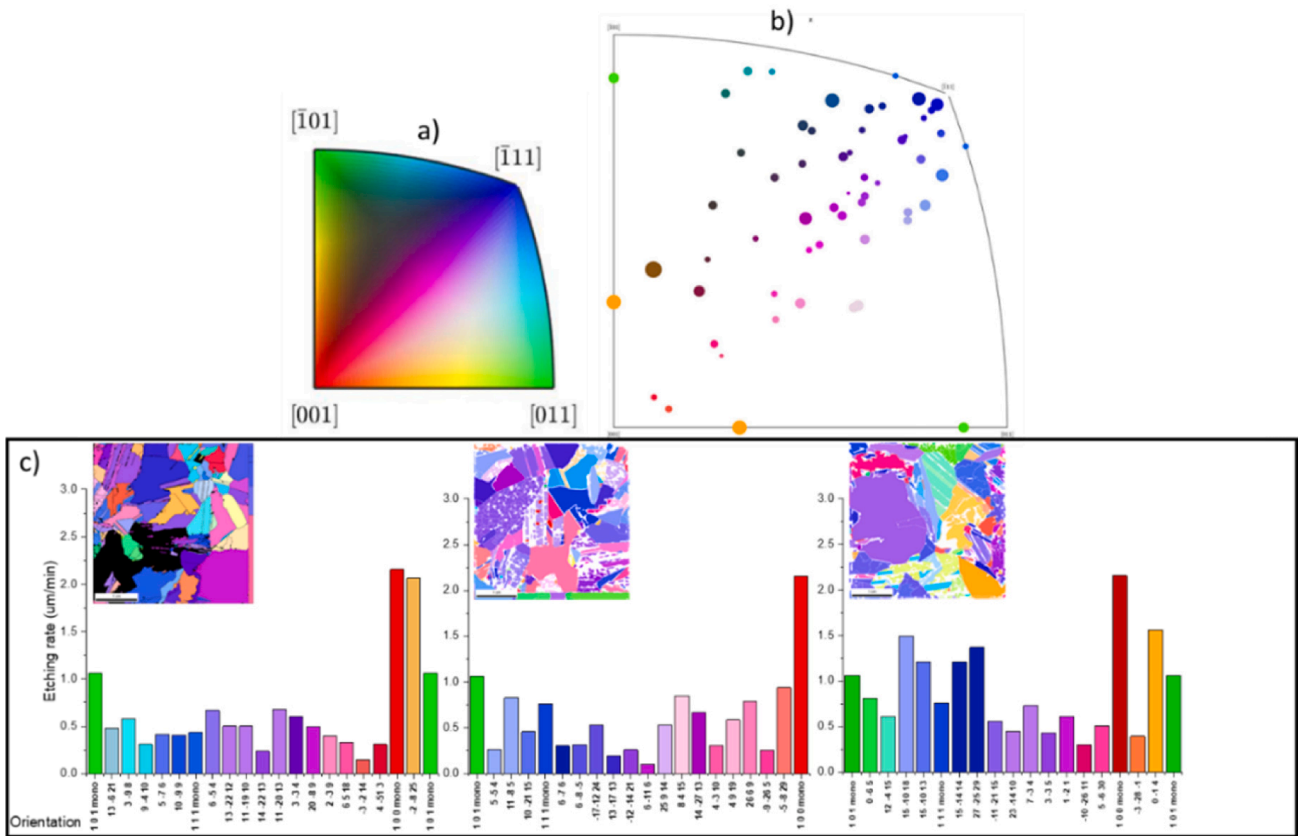
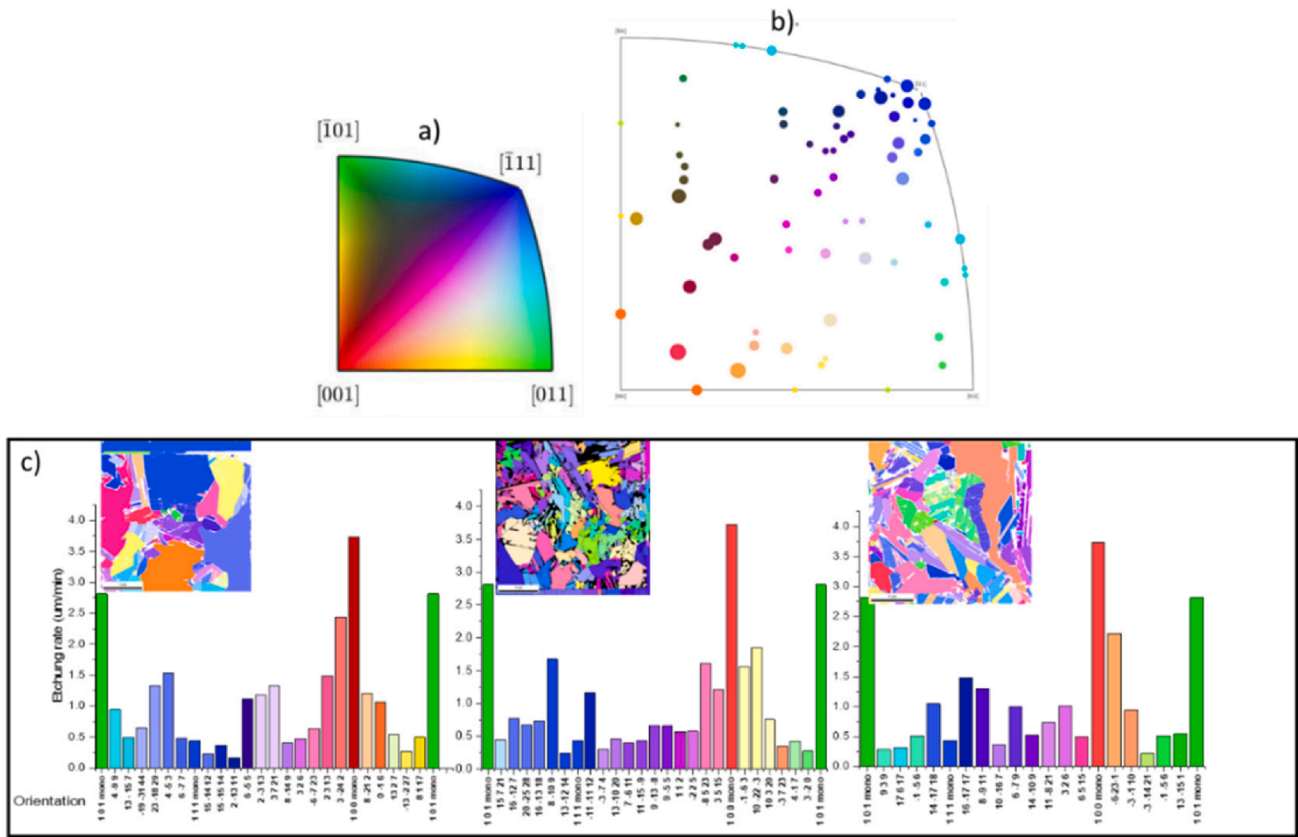


Fig. 9. a) Colour key; b) Etching rate (circle size) diagram per grain distribution for different orientations calculated from the samples; c) Etching rate per grain for each sample individually; for the recipe “KOHIPA” with 15 min etching time.



**Fig. 10.** a) Colour key; b) Etching rate (circle size) diagram per grain distribution for different orientations calculated from the samples; c) Etching rate per grain for each sample individually; for the recipe “KOHNa” with 5 min etching time.

are investigated. A detailed description of the Laue tool principle and Laue scanning process is described in our previous work [25]. An example of an optical image obtained by the Laue tool is presented in Fig. 2. The scanned data was transformed into a colour map shown in Fig. 3, using the “Orientation imaging microscopy 7” (TSL OIM analysis) software [27]. Each colour represents different crystal orientations ( $hkl$ ), allowing differentiation between grains and grain boundaries.

After crystal orientation characterization, the polished and textured samples were subjected to surface structure measurements by WLI. WLI may be used as a tool to measure height differences between the grains on the mc-wafers. SEM (scanning electron microscope) was also used to reveal the texture on the polished mc-samples. However, it cannot provide information regarding the topological height changes between grains as the plane-mode of the SEM only allows analysis of a small area ( $<1\text{mm}$ ), as shown in Fig. 5. Since WLI is still a time-consuming technique for areas over 1 cm (e.g. a  $36\times 6$  mm area analysis takes approximately 30–45 min), it was decided to scan three ( $36\times 6$  mm) areas (Fig. 3) per sample to increase the number of grains analysed for each sample. The etching rate for the different grains on the mc-wafers was calculated based on the acquired data by Equation (1):

$$\Delta h = h_{\text{unetched}} - h_{\text{etched}} \quad (1)$$

Where  $h_{\text{unetched}}$  is the morphological height of a certain area measured with WLI before etching in the corresponding texturing solution and  $h_{\text{etched}}$  is the morphological height of the same area measured with WLI after texturing. The height difference data determined by WLI before and after the etching was combined with the Laue tool maps to obtain maps of etching depth for selected grains. Following this, all data was processed in the Matlab toolbox (MTEX) to represent the etching speed and grain orientation combination [28].

$$V = \frac{\Delta h}{t} \quad (2)$$

In Equation (2),  $t$  is the etching time in a texturing solution, and  $V$  is the measured etching rate for a given texturing recipe for the multi-crystalline silicon wafers.

In the case of the mono-crystalline wafers, the etching rate was calculated by the weight difference between samples before and after the chemical etching, converted to thickness (Eq. (3)).

$$h_s = \frac{w_s}{S_s \nu_s} \quad (3)$$

$h_s$  is the thickness of the single-crystalline wafer,  $w_s$  is a wafer weight,  $S_s$  – area of the sample and  $\nu_s$  is mono-crystalline silicon density constant. Next, the difference ( $\Delta h$ ) between thickness of the etched wafer ( $h_s$ ) and before etching (as-cut)  $h_{s0}$ .

$$\Delta h = h_{s0} - h_s \quad (4)$$

Naturally, for multi-crystalline samples weight loss cannot be used to evaluate the individual crystal grain etching response as with the single crystal wafers although weight loss clearly took place as a result of etching of both mono and multi-crystalline wafers.

### 3. Results and discussion

#### 3.1. Texturing response of single-crystalline wafers

After performing experiments described in section 2.2 on the mono-crystalline wafers, the etching rate of these different orientations for the solutions “KOHNa”, “KOHIPA” and HNA were calculated and presented in Fig. 5.

As seen from Fig. 4, the solution with NaOCl additive shows a

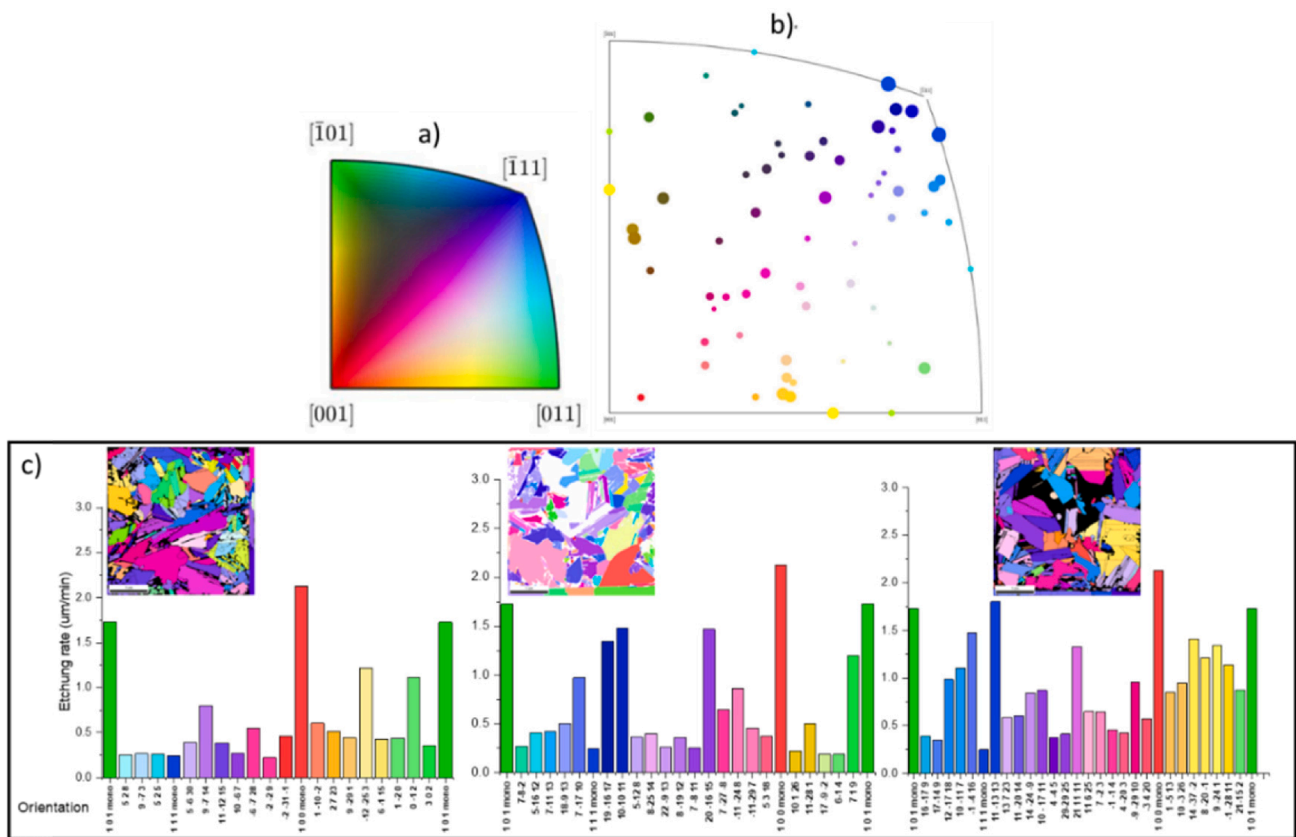


**Fig. 11.** a) Colour key; b) Etching rate (circle size) diagram per grain distribution for different orientations calculated from the samples; c) Etching rate per grain for each sample individually; for the recipe “KOHNa” with 15 min etching time.

minimal etching speed for the (111) orientation, while somewhat higher for both the (101) and (100) orientations. The IPA based solution shows the same trend as the NaOCl solution, i.e a low etching rate on the (111) orientation and increasing rates for the (101) and (100), respectively. The HNA-based solution gave the fastest and similar etching rates for all crystal orientations.

SEM micrographs of the sample surfaces of different crystalline orientations etched in solution with NaOCl and IPA are given in Figs. 5 and 6, respectively. These images support the weight measurements and clearly illustrate the different responses to the solutions. Etching with HNA solution did not give any visible effect on the surface structure, as it is acidic based etching and is hence not illustrated.

The results align with the standard KOH wet etching results of silicon in literature [29,30]. Correspondingly, the difference in the formation of microstructure for (100) and (110) orientations in the KOHIPA solution. A pyramid shaped texture was formed on the (100) orientation sample surface, while etching of the (110) orientation by KOHIPA solution resulted in a slight change of morphology. Additionally, in our case, the low pyramid density coverage of the (100) sample might be a result of hydrogen bubbles precipitation on the sample surface during etching. The cause of the formation of these hydrogen bubbles may be shortage of IPA concentration in the solution since its function is increasing the surface wetting of the immersed samples. This described role of the IPA additive appears in several studies as supportive reactive agent for improvement of Si chemical texturing [19,20,31].

### 3.2. Texturing response of multi-crystalline wafers

As will be illustrated in the following, the texturing responses for multi-crystalline wafers and the crystal orientations within these wafers, were quite different to those observed on the mono-crystalline wafers.

Structure uniformity of the entire sample surface is one of the main

challenges of wet chemical polishing or texturing processes for mc-Si wafers. As described above, “KOHIPA”, “KOHNa” and “KOHmix” recipes (Table 1) were applied on the mc-wafers to evaluate the effect of the NaOCl and IPA additives on the etching uniformity of mc-Si. However, the IPA and NaOCl additives were revealed to display not only a polishing effect (as in the mono-crystalline wafers etching), but also a surface texturing effect for the mc-wafers. SEM analysis of the etched samples combined with the Laue mapping revealed a clear texturing influence (Fig. 7), mainly on the 111 orientation grains. As described in the experimental section, the original sample thickness was different for the mono and multi-crystalline wafers, which affected the time duration that the multi-crystalline wafers could be held in the high etching-rate solution. Thus, due to the high etching rate of “KOHmix” (the mixture of IPA and NaOCl reagents), after 15 min, the samples became brittle and broke as a result of the etching. Subsequently, texturing results were not obtained for the 15 min duration in this solution.

Fig. 8 illustrates the texturing response of the “KOHIPA” recipe with 5 min etching time. We note that the planes close to the (111) orientation have the highest etching rate over other measured planes. This is in contrast to the etching rate of the single-crystalline (111) wafers under the same conditions, which displayed the lowest etching rate compared to the other three main orientations (001, 011 and 101). Such an etching effect on the mc-wafers might be related to the simultaneous etching of different grains located on a mc-wafer. Thus, it results in “equalising” of the etching rates of the different grains, despite the anisotropic etching effect of the KOH solution [12,29,32]. We can assume that a high etching rate of (100) related planes increase the etched surface area, while other planes (close to (111)) display a slower etching rate, because of the IPA additive presence, which results in the overall equalization of the etching rate for the entire mc-wafer. Fig. 9 presents additional data on the solution KOHIPA with a longer etching time of 15 min. In this case, we observe that the etching rate distribution is more



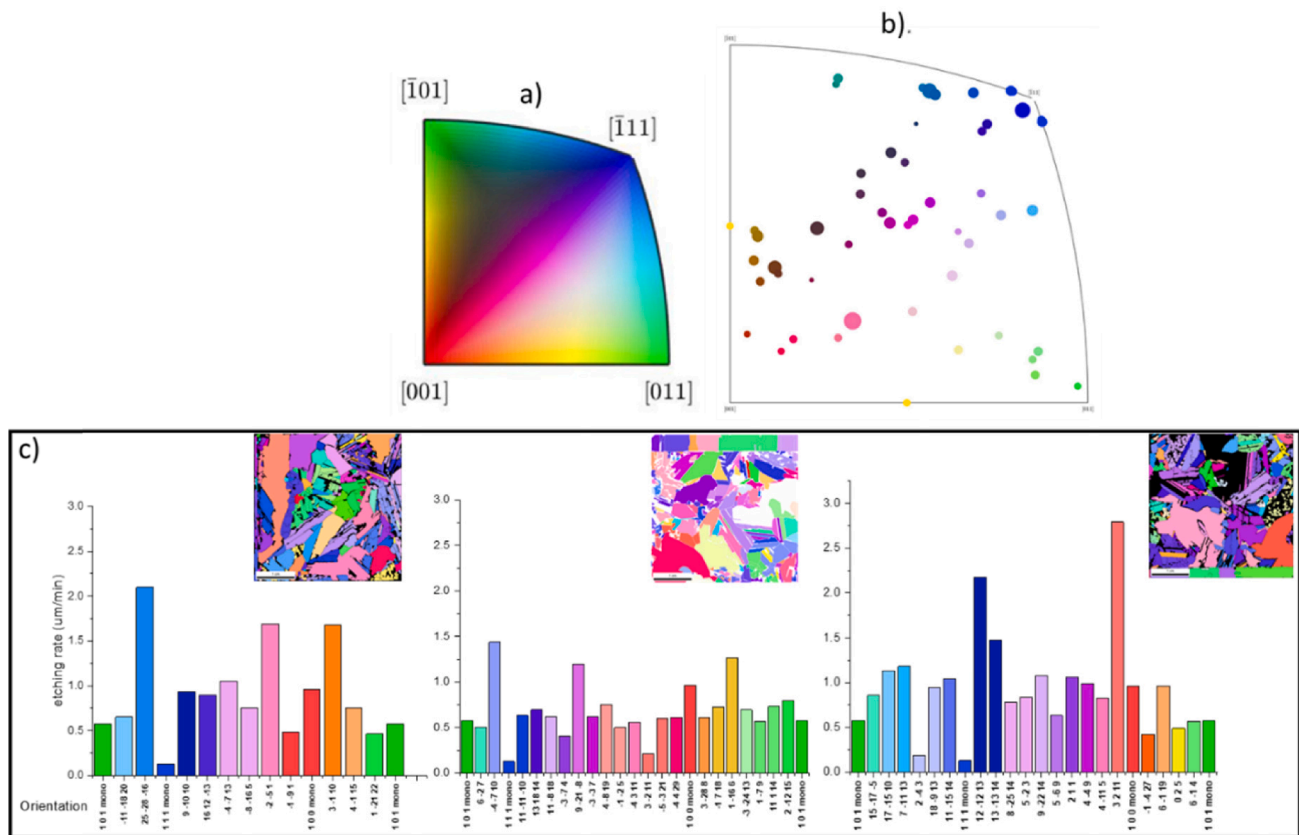


**Fig. 12.** a) Colour key; b) Etching rate (circle size) diagram per grain distribution for different orientations calculated from the samples; c) Etching rate per grain for each sample individually; for the recipe “KOHmix” with 5 min etching time.

gradual for most of the crystal planes. Thus, we conclude that for this solution (rec. “KOHIPA”), the etching of the (111) and close to (111) orientated planes have an initially higher etching rate displayed at the short etching time, while the etching rate levels off after 15 min for the different orientational planes.

Fig. 10 illustrates the etching of the mc-Si samples in the solution with NaOCl additive (recipe. “KOHNa”). We can see the same trend of the high etching rate for the planes with close to (111) orientation with a lower etching rate for other orientations for both etching times 5 and 15 min (Figs. 10 & 11). There seems to be no significant time effect for the KOHNa solution, as opposed to the KOHIPA solution showing a decreasing etching rate with time for the majority of crystal orientations.

For the solution “KOHmix” shown in Fig. 12, we see a less distinct difference of the etching speed between (101), (111), (001) and (011) planes. This can be the result of combining NaOCl and IPA additive in one solution resulting in a levelling of the etching rate for different orientations. Additionally, according to Fig. 4, the etching speed for the mono-crystalline (110 and 100) orientation wafers in the solution with NaOCl (rec. “KOHNa”) was higher than in the solution with IPA additive (rec. “KOHIPA”). This indicates that combining the additives might contribute to the homogenisation of etching rates between the main three main orientations.

In the work of Vazsonyi et al [33], a high etching rate of the (111) plane in the NaOH solution with NaOCl additive was reported. Moreover, these researchers proposed that overheating the solution above 80 °C might eliminate the etching effect of NaOCl additive. Another work of Gangopadhyay et al [34], reported high etching rate uniformity for multi-crystalline silicon at 80 °C with NaOCl additive in a NaOH etching solution. Therefore, the relatively low etching rate for the (111) orientation on the mono-crystalline wafers in our work may potentially be explained by the higher temperature, eliminating the effect of the NaOCl additive.

As illustrated by Fig. 13, the etching rate of the solution “KOHNa” is equal for different orientations, and not time dependent (5 or 15 min). Subsequently, this work concludes that the KOH solution with NaOCl additive leads to stable etching rates for mc-Si wafers. This is in accordance with the work of Gangopadhyay et al [34] that showed that the etching rate of the (111) plane is relatively similar to others planes on the sample. This finding is in contrast to the later study by Gangopadhyay et al [34] where a process temperature over 80 °C was suggested to result in NaOCl decomposition into O<sub>2</sub> and NaCl, essentially yielding a solution without NaOCl additive. Therefore, the cause of the differences between the studies may be the higher solution temperature range presented in this work.

Etching rates for all the investigated recipes have been summarised in Fig. 13. The results indicate two main trends. First, for the (111) close orientations and others, chemical etching has a slight orientational effect for separate planes on the multi-crystalline wafers. Second, in our work, etching rate distribution follows the crystallographic similarity of the hkl indexes of a certain orientation grain to the main crystallographic (100, 110, 111) planes. As a result, the etching rate is increasing towards the “edges” or the three main orientations for the KOH base wet chemical etching of the mc-Si wafers.

#### 4. Conclusions

The wet chemical etching response of multi (mc)- and mono (sc)-crystalline Si wafers to different KOH-based etching solutions was studied using a combination of LAUE X-ray crystallography scanning tool and White Light Interferometry WLI characterisation methods.

The KOH solution with IPA additive had a texturing effect on the (100) orientation of the sc-wafers, while it showed only a light morphological effect on the (110) and no effect on (111) orientations. However, all KOH based solutions had a texturing effect on the mc-Si

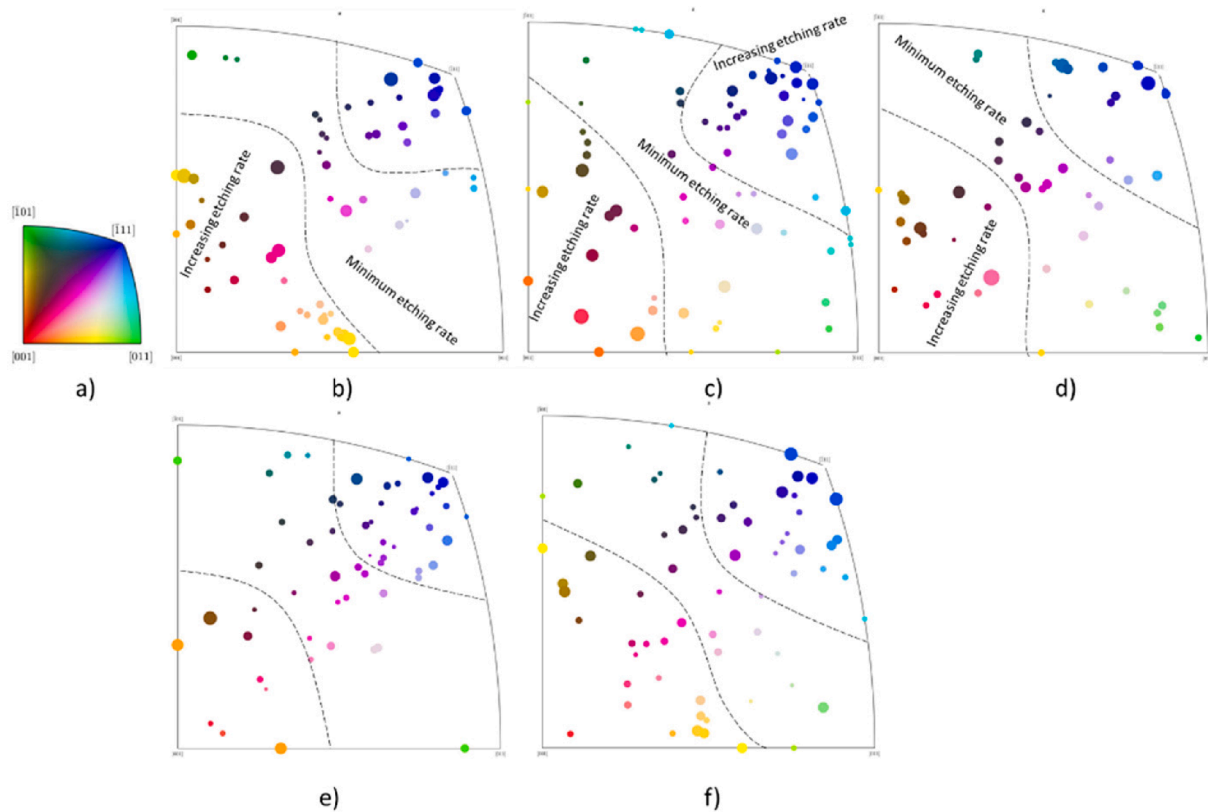


Fig. 13. a) Colour key; Etching rate (circle size) diagram per grain distribution for the different recipes and etching duration b) KOHIPA, 5 min; c) KOHNa, 5 min; d) KOHmix, 5 min; e) KOHIPA, 15 min f) KOHNa, 15 min.

samples for orientations close to (1 1 1), (1 1 0), (1 0 0). While the etching speeds for the KOH/IPA solution and KOH/NaOCl solutions were the highest for (100) orientation on the single-crystalline samples, it was the opposite for the mc-Si wafers. It was revealed that the NaOCl additive can be very effective for fast etching/polishing of the mc-Si wafers. The IPA additive has larger influence on the etching of the planes close to orientation (111), however the etching rate decreases with etching time. A uniform etching rate for all crystal orientations on mc-Si was obtained from the KOH etchant by adding both IPA and NaOCl additives. As such, this solution is considered suitable for polishing.

While the etching of the mono-crystalline Si samples is generally uniform over the whole sample surface, etching of the multi-crystalline Si samples appears to be determined by the main orientations present, especially if most crystals are close to (1 0 0), (1 1 0), (1 1 1) orientations. One of the possible reasons might be a “group affect”, as KOH solutions have anisotropic etching behaviour. Thus, the etching rate of the solution is influenced by the fastest etching orientation, creating additional directions for etching of the neighbouring grains. Moreover, a strict temperature control must be applied for wet chemical etching of mc-Si using KOH or NaOH with NaOCl additives to avoid additive decomposition and subsequent loss of etching effect.

## 5. Data availability

The raw data required to reproduce these findings can be shared if requested by the audience and reviewers.

## Declaration of Competing Interest

The authors declare that they have no known competing financial interests or personal relationships that could have appeared to influence the work reported in this paper.

## Data availability

Data will be made available on request.

## Acknowledgement

The authors gratefully acknowledge the financial support from the Research Council of Norway through the research project “DiamApp” (project no. 280831)

## References

- [1] S. Philipps, “Fraunhofer Ise, Werner Warmuth, and PSE Projects GmbH,” *Photovoltaics Report*, p. 48, 2020.
- [2] NREL, “Best Research-Cell Efficiency Chart,” ed: NREL, 2021.
- [3] T. Luka, C. Hagendorf, M. Turek, Multicrystalline PERC solar cells: Is light-induced degradation challenging the efficiency gain of rear passivation, *Photovoltaics International* 32 (2016) 37–44.
- [4] J. Bullock, M. Hettick, J. Geissbühler, A.J. Ong, T. Allen, C.M. Sutter-Fella, T. Chen, H. Ota, E.W. Schaler, S. De Wolf, C. Ballif, Efficient silicon solar cells with dopant-free asymmetric heterocontacts, *Nature Energy* 1 (3) (2016) 1–7.
- [5] M. Scherff, Novel method for preparation of interdigitated back contacted a-Si: H/c-Si heterojunction solar cells, in: *Proc. 26th Eur. Photovoltaic Sol. Energy Conf, Exhib*, 2011, pp. 2125–2129.
- [6] O. Schultz, S. Glunz, G. Willeke, ACCELERATED PUBLICATION: Multicrystalline silicon solar cells exceeding 20% efficiency, *Progress in photovoltaics: Research and Applications* 12 (7) (2004) 553–558.
- [7] T.-C. Wang, T.-H. Yeh, S.-Y. Chu, H.-Y. Lee, C.-T. Lee, Developed diamond wire sawing technique with high slicing ability for multicrystalline silicon wafers, *Materials and Manufacturing Processes* 35 (15) (2020) 1727–1731.
- [8] D. Zhao, X. Lu, Chemical mechanical polishing: theory and experiment, *Friction* 1 (4) (2013) 306–326.
- [9] Z. Zhang, J. Liu, W. Hu, L. Zhang, W. Xie, L. Liao, Chemical mechanical polishing for sapphire wafers using a developed slurry, *Journal of Manufacturing Processes* 62 (2021) 762–771.
- [10] P.K. Basu, K. Sreejith, T.S. Yadav, A. Kottanthariyil, A.K. Sharma, Novel low-cost alkaline texturing process for diamond-wire-sawn industrial monocrystalline silicon wafers, *Solar Energy Materials and Solar Cells* 185 (2018) 406–414.

- [11] U. Gangopadhyay, K.H. Kim, S.K. Dhungel, U. Manna, P.K. Basu, M. Banerjee, H. Saha, J. Yi, A novel low cost texturization method for large area commercial mono-crystalline silicon solar cells, *Solar energy materials and solar cells* 90 (20) (2006) 3557–3567.
- [12] P. Papet, O. Nichiporuk, A. Kaminski, Y. Rozier, J. Kraiem, J.F. Lelievre, A. Chaumartin, A. Fave, M. Lemiti, Pyramidal texturing of silicon solar cell with TMAH chemical anisotropic etching, *Solar Energy Materials and Solar Cells* 90 (15) (2006) 2319–2328.
- [13] B. Schwartz, H. Robbins, “Chemical etching of silicon: IV, Etching technology,” *Journal of the electrochemical society* 123 (12) (1903, 1976.) pp.
- [14] J. Ding, S. Zou, J. Choi, J. Cui, D. Yuan, H. Sun, C. Wu, J. Zhu, X. Ye, X. Su, A laser texturing study on multi-crystalline silicon solar cells, *Solar Energy Materials and Solar Cells* 214 (2020), 110587.
- [15] D. Ruby, S. Zaidi, S. Narayanan, B.M. Damiani, A. Rohatgi, Rie-texturing of multicrystalline silicon solar cells, *Solar energy materials and solar cells* 74 (1–4) (2002) 133–137.
- [16] H. Han, Z. Huang, W. Lee, Metal-assisted chemical etching of silicon and nanotechnology applications, *Nano today* 9 (3) (2014) 271–304.
- [17] J. N. Ximello Quiebras, “Wet chemical textures for crystalline silicon solar cells,” 2013.
- [18] Y. Zhang, B. Wang, X. Li, Z. Gao, Y. Zhou, M. Li, D. Zhang, K. Tao, S. Jiang, H. Ge, S. Xiao, A novel additive for rapid and uniform texturing on high-efficiency monocrystalline silicon solar cells, *Solar Energy Materials and Solar Cells* 222 (2021), 110947.
- [19] E. Abdur-Rahman, I. Alghoraibi, and H. Alkurdi, “Effect of isopropyl alcohol concentration and etching time on wet chemical anisotropic etching of low-resistivity crystalline silicon wafer,” *International journal of analytical chemistry*, vol. 2017, 2017.
- [20] W.Y. Ou, Y. Zhang, H.L. Li, L. Zhao, C.L. Zhou, H.W. Diao, M. Liu, W.M. Lu, J. Zhang, W.J. Wang, Effects of IPA on texturing process for mono-crystalline silicon solar cell in TMAH solution, in: *Materials Science Forum*, Vol. 685, Trans Tech Publications Ltd., 2011, pp. 31–37.
- [21] T. Lehmann, M. Trempa, E. Meissner, M. Zschorsch, C. Reimann, J. Friedrich, Laue scanner: A new method for determination of grain orientations and grain boundary types of multicrystalline silicon on a full wafer scale, *Acta materialia* 69 (2014) 1–8.
- [22] J.C. Wyant, “White light interferometry,” in *Holography: a tribute to yuri denisyuk and emmett leith* vol. 4737: (2002) 98–107.
- [23] K. Sreejith, A.K. Sharma, P.K. Basu, A. Kottantharayil, Etching methods for texturing industrial multi-crystalline silicon wafers: A comprehensive review, *Solar Energy Materials and Solar Cells* 238 (2022), 111531.
- [24] N. Abd Aziz, B. Bais, A. A. Hamzah, and B. Y. Majlis, “Characterization of HNA etchant for silicon microneedles array fabrication,” in *2008 IEEE International Conference on Semiconductor Electronics*, 2008: IEEE, pp. 203–206.
- [25] A.K.R. Vladyslav Matkivsky, G. Stokkan, P. Tetlie, M. Di Sabatino, G. Tranell, Novel combinatory method for surface and crystallinity analysis of crystalline materials, *MethodX* (2022).
- [26] S. Zhang, F. Meng, R. Söndenå, Z. Liu, G. Tranell, Investigation of nanoscale quasi pyramid texture for HIT solar cells using n-type high performance multicrystalline silicon, *Energy Procedia* 124 (2017) 321–330.
- [27] EDAX, “OIM Analysis,” ed, 2018, p. <https://www.edax.com/>.
- [28] F. Bachmann, R. Hielscher, H. Schaeben, Texture analysis with MTEX-free and open source software toolbox, in: *Solid State Phenomena*, vol. 160, Trans Tech Publ, 2010, pp. 63–68.
- [29] O. Powell, H.B. Harrison, Anisotropic etching of 100 and 110 planes in (100) silicon, *Journal of Micromechanics and Microengineering* 11 (3) (2001) 217.
- [30] S. Campbell, K. Cooper, L. Dixon, R. Earwaker, S. Port, D. Schiffrin, Inhibition of pyramid formation in the etching of Si p (100) in aqueous potassium hydroxide-isopropanol, *Journal of Micromechanics and Microengineering* 5 (3) (1995) 209.
- [31] I. Zubeľ, K. Rola, M. Kramkowska, The effect of isopropyl alcohol concentration on the etching process of Si-substrates in KOH solutions, *Sensors and Actuators A: Physical* 171 (2) (2011) 436–445.
- [32] K.E. Bean, Anisotropic etching of silicon, *IEEE Transactions on electron devices* 25 (10) (1978) 1185–1193.
- [33] É. Vázquez, Z. Vértessy, A. Tóth, J. Szlufcik, Anisotropic etching of silicon in a two-component alkaline solution, *Journal of Micromechanics and Microengineering* 13 (2) (2002) 165.
- [34] U. Gangopadhyay, S.K. Dhungel, K. Kim, U. Manna, P.K. Basu, H.J. Kim, B. Karunakaran, K.S. Lee, J.S. Yoo, J. Yi, Novel low cost chemical texturing for very large area industrial multi-crystalline silicon solar cells, *Semiconductor Science and Technology* 20 (9) (2005) 938.